International Conference
ENGINEERING MECHANICS 2010
Svratka, Czech Republic, May 10 – 13, 2010

INVESTIGATION OF FLOW STRUCTURES IN A CYLINDRICAL CAVITY USING TIME-RESOLVED PIV AND POD ANALYSIS

P. Procházka*, K. E. Meyer**

Summary: *The flow structures inside a cylindrical cavity are studied experimentally using time-resolved PIV. The flow is excited using rotating lid controlled by step motor. POD analysis is used as a filter as well as a method to detect the structures inside the fluid. Observed POD modes are ordered in terms of relative energy. Investigation is performed in horizontal plane for wide range of Reynolds number.*

1. Introduction

For this experiment data were sampled using time-resolved Particle Image Velocimetry (PIV) that can be used to detect not only instantaneous flow structures, but also frequencies associated with the flow structures. Data for frequency investigation should meet Nyquist criterion, i. e. data must be sampled with frequency at least two times higher than the highest frequency which is presented in the signal. This requirement demands much bigger sample frequency then frequencies in the field of interest. Another problem is that PIV has quite big level of noise and that tight light budget is very often another source of even greater noise. That seems to be a problem in studies of flow instabilities. There is a need to use some kind of filter in time as well as in space. Proper Orthogonal Decomposity (POD) seems to be a good help as both a filter and as a method for investigation of flow structures and associated frequencies.

We used time-resolved PIV to study flow instabilities inside a flow in a cylindrical cavity with a rotation top lid. This kind of flow is well-known for generating axisymmetric vortex breakdown for a long time. Recently, non-axisymmetric flow structures have been identified and new type of POD modes are still discovered in the present.

There are not so distinct variations between mean flow and snapshots inside the flow and it is not easy to detect them. They are almost identical to the mean flow. The variations are often in order of magnitude of PIV noise. Using POD analysis the flow structures are determined by the POD modes as vortex or as pairs of vortices placed azimuthally. The vortices rotate around axis of the cylinder cavity with a rotation speed different from the speed of the lid. By increasing lid rotation Reynolds number increases and new POD modes appear and replace each other.

* Ing. Pavel Procházka: Ústav mechaniky tekutin a energetiky, Fakulta strojní, České vysoké učení technické v Praze; Technická 4; 166 07 Praha 6; e-mail: pavel.prochazka1@fs.cvut.cz
** Knud Erik Meyer, Ph.D.: Department of Mechanical Engineering, Technical University of Denmark; Nils Koppels Alle 403; 2800 Kgs. Lyngby; e-mail: kem@mek.dtu.dk

2. Experimental setup

The experiment was carried out in a cylindrical cavity made from a plexiglass pipe with an inner diameter 288 (R=144 mm). There was a glass window on the bottom of the cavity and the top was a plexiglass lid that could be rotated using step motor and gear with belt. The gap between the lid and the cylinder wall was 0,3 mm. The height of the lid over the cylinder bottom was adjustable but for all time this distance was H=3R. The hollow pipe connected the lid with gear that allowed taking a sample of fluid. One rotation of the lid corresponded to 1200 steps. The working mixture was water with glycerin in some rate. Since the viscosity is depended very strongly on the temperature there was a need to do a widely measurement of the viscosity. Due to ensuring temperature-steady conditions the cavity was placed inside a rectangular glass box (0,7x0,7x0,8 m) filled by fresh tap water. Then the box kept down the optical aberrations too.

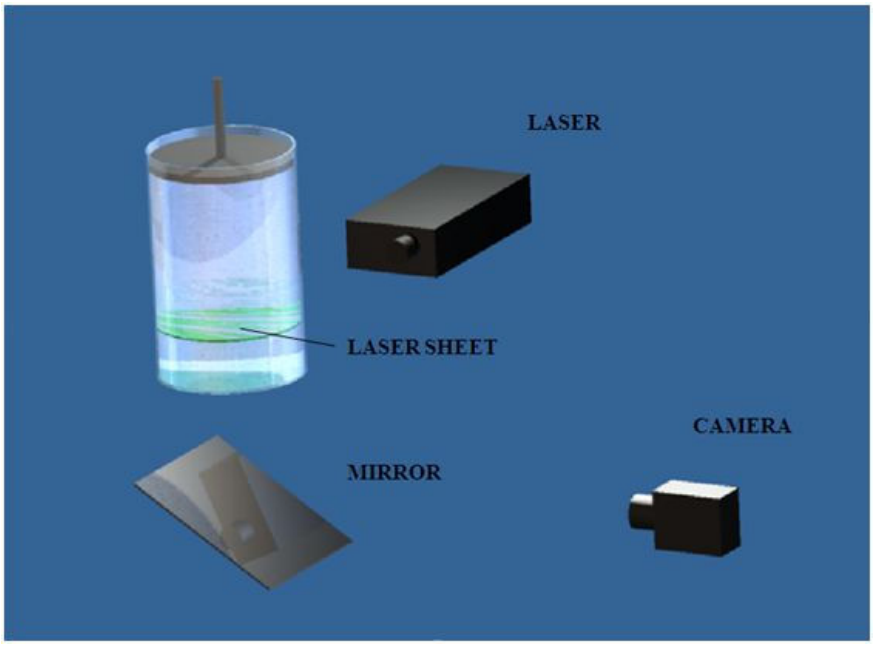

Fig. (1) – arrangement of experiment

The working fluid was seeded with silver-coated hollow particles with average diameter of 5 μm. But some dye and some gross dirt particles were presented in the mixture from previously measurements, which was a good challenge for PIV.

Due to providing convenient optical path of the camera the mirror was placed under the box with the cavity inside and the camera was on the stand in some distance horizontally from the cylinder.

The PIV system was from Dantec Dynamics A/S and consisted of New Wave Solo 120XT (120 mJ dual cavity Nd:YAG) and HiSense MKII camera. The resolution of this camera was 1344x1024 and it was used with objective Nikon 60 mm with an F-number of 2,8. The laser stand was placed so that a laser sheet was perpendicular to the cylinder axis. The stand allowed to adjust the height of the sheet and in some range the other two movements.

The Reynolds number (Re) of the flow is defined as

$$Re = \frac{\Omega R^2}{\nu} \qquad (1)$$

where ν is kinematic viscosity, R is inner radius and Ω is angular velocity of the lid. By increasing the velocity Re has been becoming greater.

Data was acquired and processed on a PC with Dynamics Studio version 2.21. For all cases the processing consisted of adaptive correlation with interrogation area 32x32 pixels, overlap 50% for both directions, number of steps was set to 2. Validation used local median of neighborhood size 3x3 and acceptable factor was 0,1.

3. POD analysis

For the analysis of the flow structures "snapshot POD" was used. Each instantaneous PIV measurement is considered as a snapshot in this case. The mean flow was calculated from all snapshots. The mean flow is presented here as the 0. mode. Then all snapshots were subtracted from mean flow resulting in the fluctuating part of the snapshots denoted with the velocity components (u, v). Then a matrix was created and defined as

$$\boldsymbol{U} = [\boldsymbol{u}^1\ \boldsymbol{u}^2\ \ldots\ \boldsymbol{u}^N], where\ \boldsymbol{u}^1 = [u_1^1 \ldots u_{lm}^1\ v_1^1 \ldots v_{lm}^1]^T \quad (2)$$

that has N columns and each snapshot is arranged in one column. The autocovariance matrix $\tilde{C} = U^T U$ is calculated and the corresponding eigenvalue problem is solved using equation $\tilde{C}A^i = \lambda^i A^i$, where λ^i is vector of eigenvalue and A^i is eigenvector.

The solutions were arranged by eigenvalues as $\lambda_1 > \lambda_2 > \ldots > \lambda_N > 0$. The ordering of eigenvalues by magnitude ensured that the most important POD modes in terms of energy were the first modes. The POD modes were then calculated as:

$$\emptyset_i = \frac{\sum_{n=1}^{N} A_n^i \boldsymbol{u}^n}{\left\|\sum_{n=1}^{N} A_n^i \boldsymbol{u}^n\right\|}, \quad \text{i=1,...,N} \quad (3)$$

A reconstruction coefficient could be found by multiplication particular snapshot by each of the POD modes $a_i = \emptyset^i \boldsymbol{u}^n$ and snapshot could be reconstructed using these coefficient as: $\boldsymbol{u}^n = \sum_{i=1}^{N} a_i^n \emptyset^i$.

The amount of total kinetic energy from velocity fluctuations in the snapshots is proportional to the corresponding eigenvalue. So the first modes are associated with higher rate of relative energy and thus with larger scale flow factor. Dominant flow structures are then reflected in the first modes.

4. Viscosity measurement

Firstly the sample of working mixture was obtained from the cavity using a syringe and tiny pipe conducted through the driving tube. The capillary viscometer was used for this measurement. It was cleaned and dried because of occurrence unwelcome particles. The viscometer with the sample inside was inserted into a small aquarium with tap water. The temperature of water was kept a distinct value using mixture of a propeller. The investigated temperatures were 20, 23, 26 and 29 °C. For each point three separately measurements were performed. Then the viscosity was calculated as an average of these.

The efflux time when the liquid level of the sample flew down from the start mark to the final mark was multiplied by viscometer constant resulting in kinematic viscosity. The result

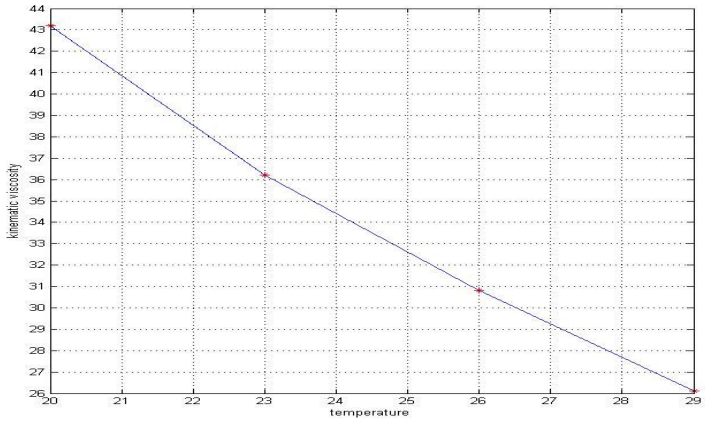

Fig. (2) – temperature-kinematic viscosity relationship

is shown in Fig. 2. One can clearly see how the kinematic viscosity decreases with temperature.

5. Measurement procedure

The space of measurement was perfectly covered with black blankets including laser. There was only one orifice for camera view. For given Re numbers it is important to know revolution of step motor – steps. The definition of Re number was mentioned previously and $\Omega = 2\pi f$. By modification of these equations the frequency is given as

$$f = \frac{Re\nu}{2\pi R^2} \qquad (4)$$

By multiplication by 1200 we can get a relationship between Re number and steps of motor.

The adjustment of time between pulses was determined by the velocity of flow. Hence time between pulses was set for each measurement cycle individually. A few test measurements were performed before main set of measurement.

The first test should have shown if there is any internal memory of flow – if there is an influence how certain Re number is reached (for example Re=3200 can be reached from Re=3000 by increasing or from Re=3400 by decreasing). But we found only small deviations in these two ways so for the next time only increasing of velocity was used.

The second test measurement was performed in two different levels of height of laser sheet. After that there was a decision to do the main measurement in height of H/4 which corresponded with distance of 108 mm from the bottom of the cylinder. This final measurement was performed in temperature of 21,2 °C which is appropriate $\nu=40{,}3\cdot10^{-6}$ m^2/s. Trigger (sample) rate was 6 Hz and number of images was 1500 for each Re number. The measurement took place for range of Re number from 2800 to 4500 with step of 100 and then from 4500 to 6300 with step of 200. There was a break of 10 min due to adaptability of flow to new velocity conditions between each series and then the new cycle has begun.

After that transient measurement was done which should have shown the behaviour of the flow in transient time between two different speeds of the lid. But no new modes were detected inside this not-steady flow.

6. Results and discussion

No instabilities were detected for Re=2800 and below, i. e. POD modes were with no systematic patterns and relative energy was almost equal for all modes. The first type of mode was discovered for Re=2900 and appeared in the first two modes. One can see a pattern consisted of 4 pairs of vortices placed axisymmetric and close to the wall. This mode is denote to be of type k=4. The lowest Re number where two different types of POD modes were observed was Re number of 3000. Figure 3 shows a snapshot and fluctuation part from this cycle. It is difficult to recognize any systematic pattern from fluctuations. Fortunately, POD analysis can identify modes and associated frequencies.

Figure 4 shows the first three POD modes observed for Re=3200. The first two POD modes represented four pars of vortices (were denoted k=4) and were identical, but displaced half a vortex length from each other. This is similar to sine and cosine function and one can see this from the time variation of the reconstruction coefficients. Fig. 4c shows the third POD mode. This represented one vortex axisymmetric with the axis and is denoted to be of type k=0. This mode is consistent with the oscillating vortex breakdown. Fig. 4d shows distribution of the relative energy of POD modes. The first two have together about 40% of the total energy and are dominating. The other mode has 13% but it is still significantly larger in energy then the following modes.

Figure 5 shows other types of POD modes. Fig. 5a shows a mode with two counter-rotating vortices with center located very closely to the center of the cylinder. It is denoted to be of type k=1. There were some combination of mode k=1 resulting in case with one of these two vortices much weaker. For higher Re number there was just velocity field going through the center and these two vortices were atrophy. However these POD modes contained more or less noise. Another POD mode is similar like Fig. 5a but is rotated 90°. Figure 5b shows POD mode with 5 pairs of vortices and is denoted to be of type k=5. Figure 5c shows POD mode with 6 pairs of vortices and is denoted to be of type k=6. There were POD mode denoted to be of type k=7 and k=8 also. However POD mode k=8 contained quite big noise. A symmetrical pattern consistent two or three pairs of vortices were observed in a few POD modes but always with low rate of energy. Some POD modes could not be detected because they appeared with quite a bit of noise.

There were a lot of combinations of POD modes. Nevertheless, only some of them could be recognized clearly and denoted. One of them is at the Fig. 5d and it is a variation of mode type k=4. It consists of an inner and an outer ring of vortices and is associated with frequency that is different from frequency of type k=4. It is denoted to be of type k=4’ and was observed from Re=3800 to Re=4000. Another example of combination is at Fig. 5e.

Figure 6 shows an analysis of all observed modes in terms of relative energy. There is a sum of the relative energy of a specific mode type as a function of the Re number. This allows to learn which mode type is dominating for certain Re number. The legend shows which symbol belongs to each mode type. One can clearly seen that the most dominant mode type are k=0 and k=4. The first mode type that appears for Re number from 2900 is k=4 with high rate of energy associated but immediately starts to decrease. Mode type k=0 appears a little bit later from Re number about 3000 and immediately increases in relative energy until Re number about 3500. After that this mode type decreases and mode type k=4 increases again and become the most important mode type. Mode type k=0 continues in slowly decreasing. Mode type k=4 decreases again from about 3800 but has still much more relative energy then k=0. However, from Re number of 4700 this mode type falls down below 10 % of relative energy

a) b)

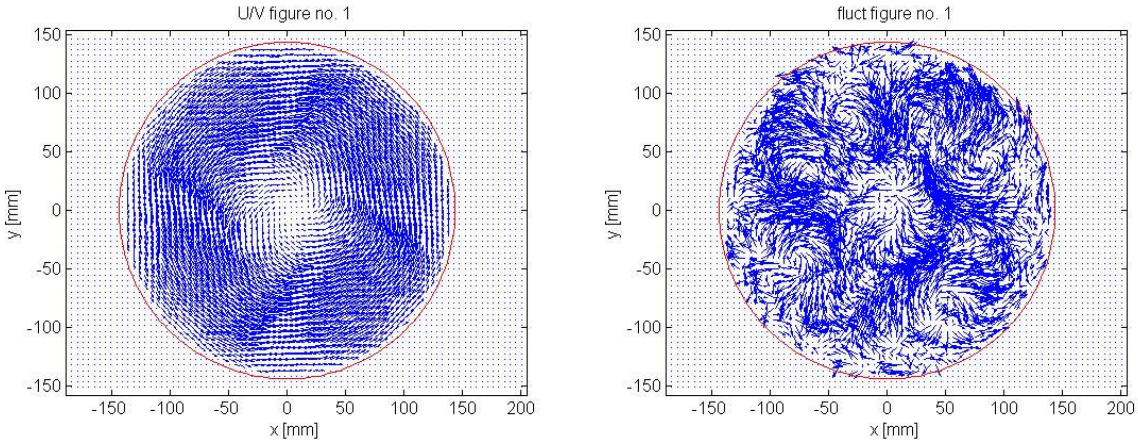

Fig. (3) – snapshot and fluctuation part (another scale) for Re=3000

a) b)

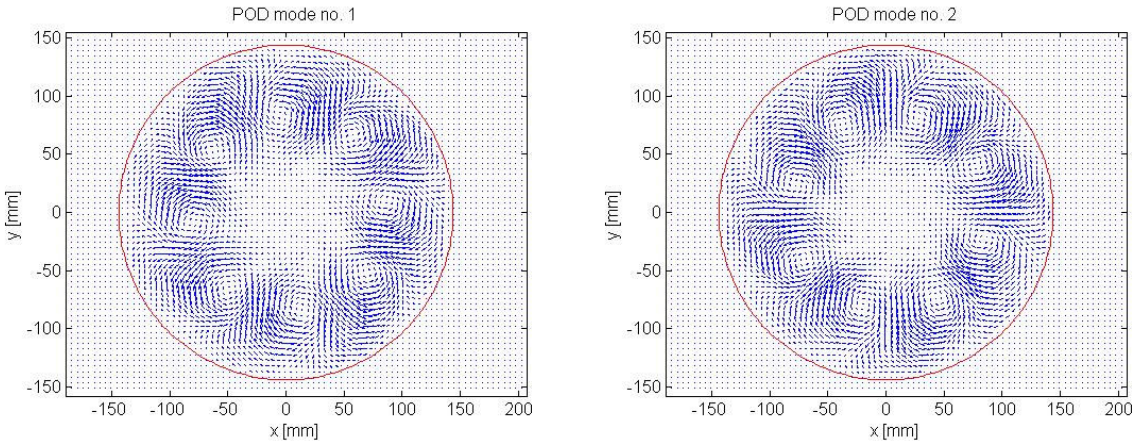

a) b)

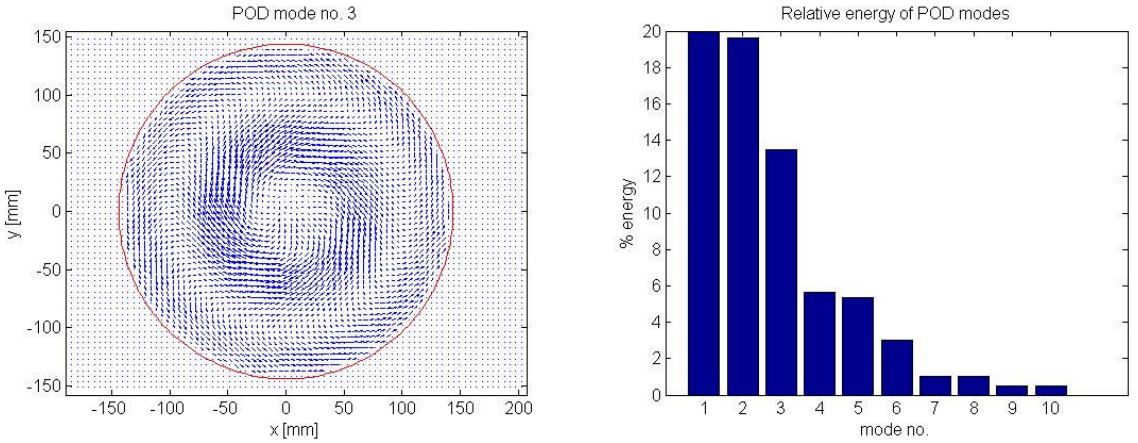

Fig. (4) – the first three POD modes and relative energy for Re=3200

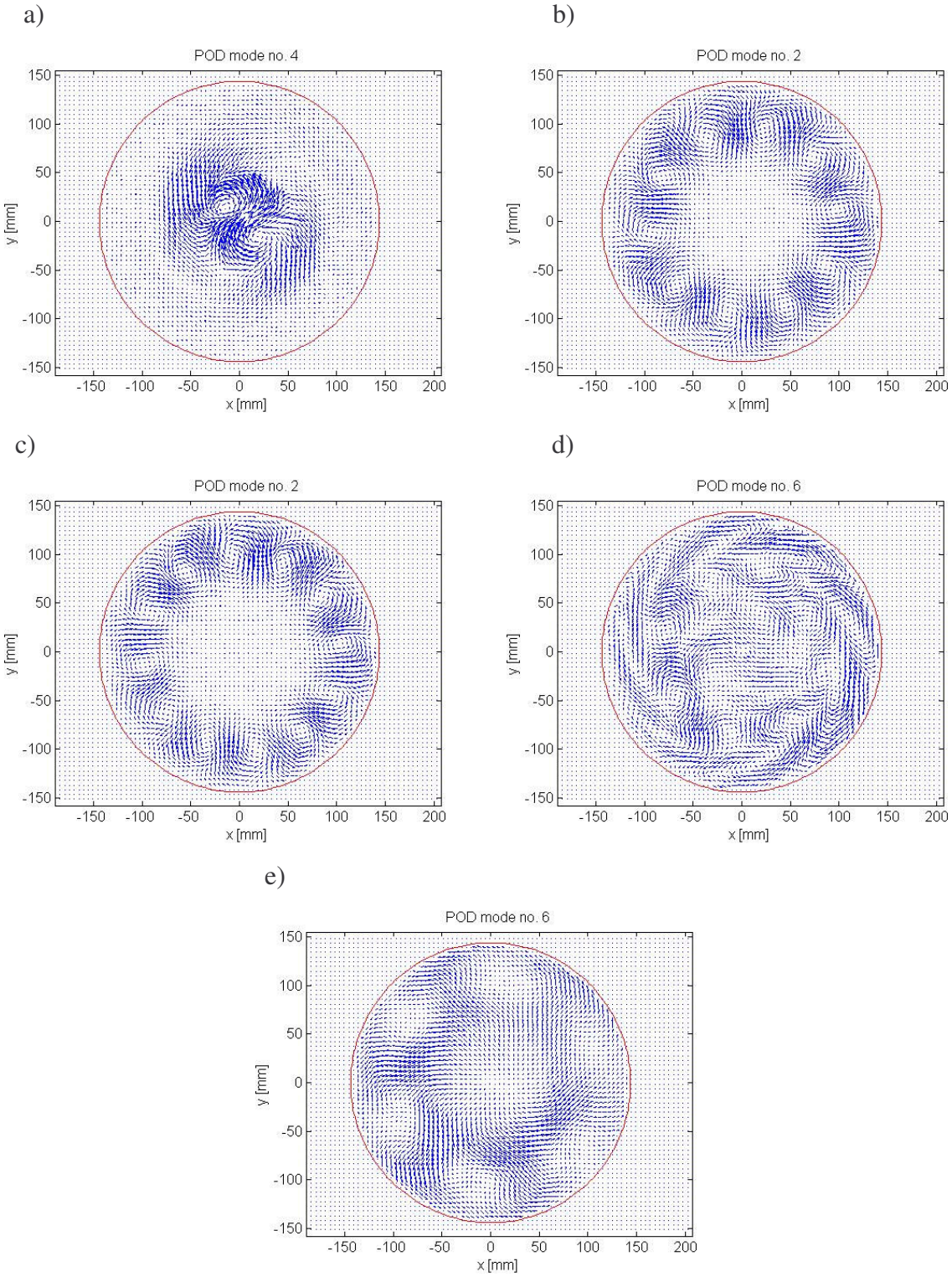

Fig. (5) – examples of mode types k=1, k=5, k=6, k=4’ and mode combination

and from Re=5700 disappears forever. From Re=4800, mode type k=5 seems to replace mode k=4 and new mode types k=6 and k=7 appear.

Quite important mode type is k=1. This appears at Re=3000 and its maximum seems to be at Re number about 3200 and after Re=4000 disappears. From Re=5000 there are some new mode types (k=6, k=7, k=8) and some combinations of modes. Consequently, each mode type loses its relative energy and there is no dominant mode type from Re=6000.

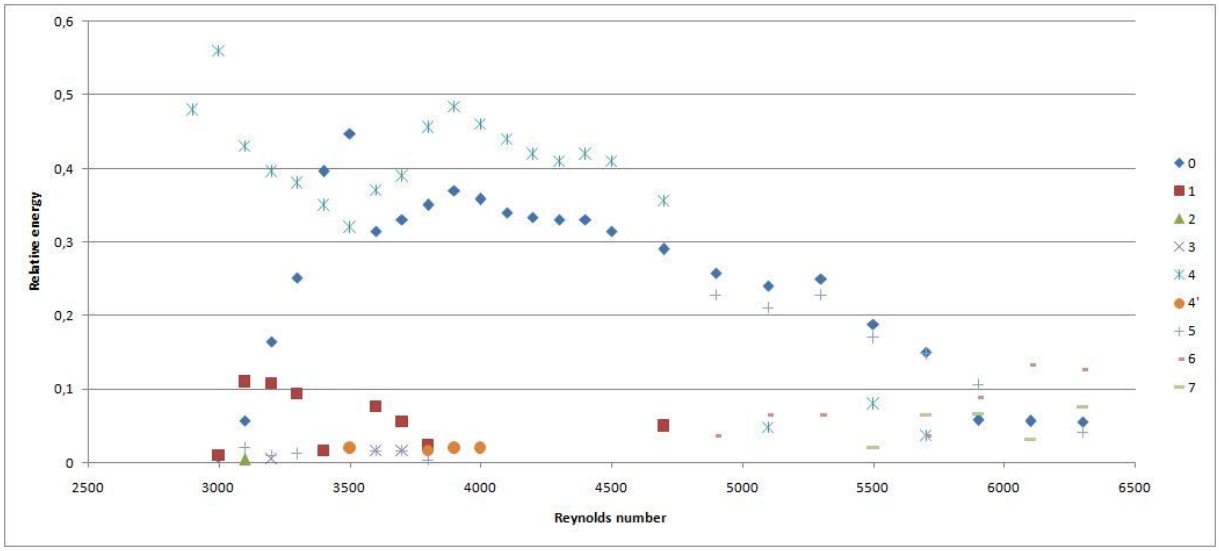

Fig. (6) – relative energy of a specific mode type as a function of the Re number

7. Conclusions

It is quite impossible to see some systematic patterns in fluctuation vector maps but POD analysis can easily identify POD modes, associated frequencies and can order them in terms of relative energy. For this time one can summarize a few results.

There is no instabilities in the flow for Re=2800 and less. The flow structures appear as vortices; either one vortex or pairs of vortices. More or less, every pattern of vortices seems to be axisymmetric to the axis. From Re=2900 four pairs of vortices are as the first mode. From Re=3400 only one vortex seems to be the first POD mode, the second and the third mode is type k=4. Five pairs of vortices replace four pairs from Re=4900 and from Re=6100 there are six pairs. The energy of the first modes decrease with Re number and from approximately Re=5700 there is no overweight of the first three modes in compare with others.

For the next time, there will be a special investigation of frequencies associated with distinct mode type to learn widely relationships between all POD modes, how they create, how they disappear and cooperate each other.

8. Acknowledgement

The authors gratefully acknowledge financial support of the Grant Agency of the Czech Republic, project No. 101/08/1112.

9. References

Meyer, K. E., Sørensen, J. N., Mikkelsen, R. & Watz, B. B. (2008) Frequency and flow structures detection in a cylindrical cavity using POD. In R. J. Adrian *et al*, editor, *14th Int. Symposium on Applications of Laser Techniques to Fluid Mechanics,* Lisbon, Portugal

Uruba, V. & Knob, M. (2008) Application of the Orthogonal Decomposition Method. In *22nd Symposium on Anemometry,* Holany, Czech Rep., pp. 103-108

10. Appendix

Tab. (1) – table of the first four POD modes for every investigated Reynolds number

Re\No.	1	2	3	4	rel. energy of the first four modes [%]
2800	-	-	-	-	-
2900	k=4	k=4	-	-	24/23/0/0
3000	k=4	k=4	-	k=0	29/28/1/1
3100	k=4	k=4	k=1	k=1	22/21/6/6
3200	k=4	k=4	k=0	k=1	20/20/13/5,5
3300	k=4	k=4	k=0	k=0	19/19/18,5/5
3400	k=0	k=4	k=4	k=0	23/18/17,5/10
3500	k=0	k=4	k=4	k=0	25/16/16/14
3600	k=0	k=4	k=4	k=0	27/19/19/4,5
3700	k=0	k=4	k=4	k=0	28/20/20/5
3800	k=0	k=4	k=4	k=0	30/23/23/5
3900	k=0	k=4	k=4	k=0	31/24/24/5
4000	k=0	k=4	k=4	k=0	30/23/23/5
4100	k=0	k=4	k=4	k=0	28/22/22/5
4200	k=0	k=4	k=4	k=0	28/21/21/5
4300	k=0	k=4	k=4	k=0	27/21/21/5
4400	k=0	k=4	k=4	k=0	27/21/21/5
4500	k=0	k=4	k=4	k=0	26/20/20/5
4700	k=0	k=4	k=4	k=0	23/18/18/6
4900	k=0	k=5	k=5	k=0	20/11/11/5,5
5100	k=0	k=5	k=5	k=0	18,5/10,5/10,5/5
5300	k=0	k=5	k=5	k=0	19/8/8/6
5500	k=0	k=5	k=5	k=0	13/8,5/8,5/6
5700	k=0	k=5	k=5	k=0	10/5,5/5,5/5
5900	k=0	k=5	k=5	k=6	6/5,5/5,5/4,5
6100	k=0	k=6	k=6	-	5,5/5/5/4
6300	k=0	k=6	k=6	k=6	5,5/4/4/4